

NEAR-SURFACE RESULTS OF ACTIVE SEISMIC TRANSECTS OF THE RIM AND CRATER OF THE KILBOURNE HOLE, NM MAAR VOLCANIC CRATER. J. Wang¹ (jcwang1@umd.edu), N. Schmerr¹, E. Bell^{1,2,3}, N. McCall², L. Wike¹, J. Richardson², J. West⁴, S. Rees⁵, C. Braccia¹, C. Barry², J. Hurtado⁶, T. Sweeney⁶, N. Valenzuela⁶. ¹UMD, College Park, MD; ²NASA GSFC, Greenbelt, MD; ³CRESST, Greenbelt, MD; ⁴Arizona State University, AZ; ⁵Navarro Research and Engineering; ⁶University of Texas, El Paso.

Introduction: Maar volcanic craters form from highly volatile eruptive centers and typically have central craters that are surrounded by a low profile tuff ring of pyroclastic material deposits [1]. This style of eruption excavates materials throughout the crustal column providing an opportunity to study the subsurface composition and volatile content of the crust near the eruption. The study of terrestrial maar craters, as analogs to those on the Martian surface, can increase our understanding of Martian volcanism, crustal structure, and the past presence of volatiles.

In November of 2021 and in April of 2022, the NASA SSERVI GEODES and RISE2 teams collaborated at Kilbourne Hole, NM, a maar volcanic crater within the Potrillo Volcanic Field (PVF) [2]. During these field expeditions, the GEODES team conducted geophysical surveys of both the crater rim and within the crater itself.

Geologic Background and Study Objectives:

Kilbourne hole has previously been used as a training site for Apollo astronauts and continues to be an important site for exploration simulations and planetary analog studies. Kilbourne Hole, formed in the mid-Pleistocene, is one of several maar volcanic craters that are found within the Potrillo Volcanic Field, NM [3]. The rim of Kilbourne Hole is constructed of four primary strata. From upper to lower, these strata consist of an ash deposit, a surge bed, a basaltic lava flow, and bottom fluvial sedimentary rocks. The central crater subsurface hosts alluvium and reworked volcanic deposits with diabase dikes and diatreme filling in the deeper subsurface [5].

The objectives of our study are to 1) coordinate a co-located multi-geophysical-technique investigation of Kilbourne Hole rim strata [2], and 2) geophysically constrain the interior structure of the crater and rim. As part of our 2021 geophysical investigation, four active seismic geophone transects were completed; one transect at the surface of each of the primary strata layers [4]. The central crater of Kilbourne Hole has previously been surveyed with magnetic and gravimetric methods, with the resulting analysis showing several dikes intruding into the crater diatreme [5]. Our 2022 field work targeted the dikes proximal to the crater center to better constrain their depth, as well as the overall structure of the diatreme deposits. Additionally, we examine the strata at the base of the rim within the crater.



Figure 1. Google Earth view of Kilbourne Hole. Stars indicate locations of seismic transects with three parallel rim seismic transects (Lines 1-3) shown in inset.

Methods & Analysis:

Refraction Analysis. We use the results of a seismic refraction analysis alongside reflection data processing, which provides us with a baseline velocity model with depth. Our refraction code utilizes a transdimensional hierarchical Bayesian framework implementing a reversible-jump Markov Chain Monte Carlo code [6, 7, 8]. Seismic data is first analyzed in Pickwin [9] for first arrival and velocity estimates, before being ingested into the refraction code.

A preliminary subsurface velocity model is shown in Fig. 2a, with three distinct velocity zones corresponding to the expected velocity ranges for loose ash deposits, more compressed surge beds, and a basaltic lava flow. We assume flat topography, which is roughly accurate for the crater rim, and encounter a low velocity zone below the basalt layer. Thus, this model can be utilized to estimate velocity with depth to the basalt layer alone, at about 20 m below the surface.

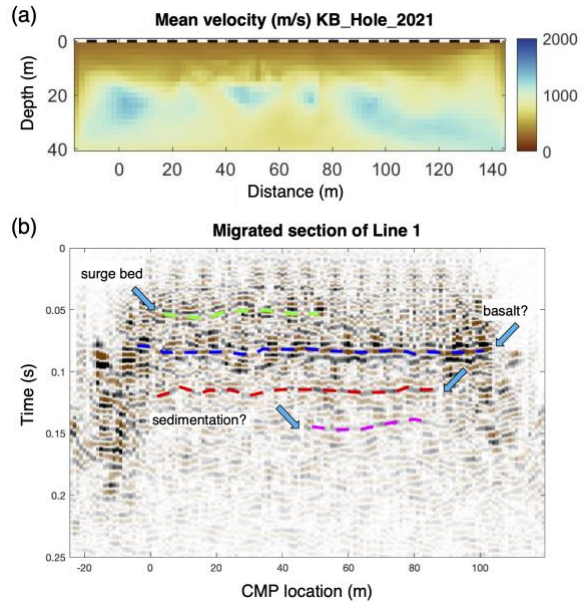


Figure 2. (a) 2D refraction velocity inversion for the subsurface structure below Line 1. (b) The reflection seismic section along Line 1.

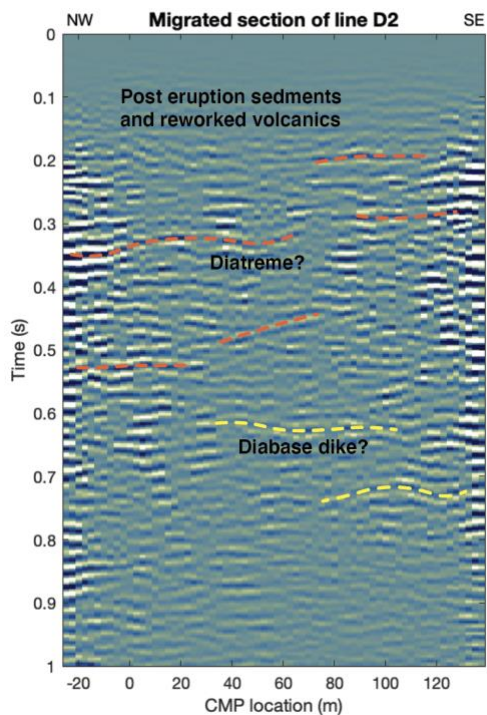


Figure 3: Migrated seismic profile along inner crater line D2.

Reflection Analysis. We present six seismic reflection profiles, two within the crater and four from the crater rim (Fig. 1).

The seismic survey along the rim consists of four geophone lines. The data was acquired along each line using variable (8-16 m) shot spacing and 2 m receiver

spacing with 48 14 Hz geophones. An additional two seismic lines from within the crater were acquired in April 2022. These profiles are 115 m long, we used 24 14.5 Hz geophones with 10 m shot spacing and 5 m receiver spacing, with additional offset shots every 10 m extending to 50 m before and after the profile line. Lines from the rim and crater center both used an aluminum base metal plate with a 20 lb sledgehammer as the seismic source.

The primary objective of reflection data processing is to enhance coherent reflections due to geologic boundaries. The data are processed using the CREWES MATLAB toolkit [10]. The raw shot gathers are preprocessed by removing bad traces, top muting, amplitude scaling, and trace equalization. To attenuate the dominant low-frequency surface waves, we apply both bandpass filtering and linear Radon transform. The filtered shot gathers are then sorted into common midpoint (CMP) gathers. We perform semblance analysis for stacking velocities used in the normal moveout (NMO) correction. Finally, we apply Kirchhoff migration to the NMO-corrected stacks using the stacking velocity model.

The reflection section from Line 1 reveals different geologic units (Fig. 2b). The seismic event observed at ~0.05 s is interpreted as the reflection resulting from the surge bed. The strongest reflector at ~0.08 s is likely related to the basalt layer, which corresponds to the refraction velocity contrast at 20 km depth. As a next step, we will work towards time-to-depth conversion based on the velocity model from refraction tomography.

Line D2 is from the central region of the crater, directly over a diabase dike. This section shows several reflections, possibly resolving the dike, the surrounding diatreme and post eruption sediments (Fig. 3).

Conclusions: Our seismic sections resolve refractions (Fig. 2a) and reflections which we interpret as the surge deposit, basalt flow (Fig. 2b) and subsurface structure in the crater center (Fig. 3).

Acknowledgements: Thank you to the NASA SSERVI GEODES and RISE2 nodes for the opportunity to participate in this research.

References: [1] White & Ross (2011), *Journal of Volc. and Geotherm. Res.*, [2] Schmerr, et al. (2022), NESF 2022. [3] Seager (1987), *New Mexico Geology*. [4] Wike, et al. (2022), NESF 2022. [5] Maksim (2016), *Dissertation, UTEP* [6] Huang, et al. (2021), *Geochem., Geophys., Geosys.* [7] Rawlinson, et al. (2005), *Exploration Geophy.* [8] Sambridge, et al. (2006), *Geophy. Journal Int.* [9] SeisImager/2D. (2009). [10] Margrave & Lamoureux, (2019), *Cambridge Uni. Press.*